

Iris image selection and localization based on analysis of specular reflection

Soumyadip Rakshit and Donald M. Monro
Department of Electronic and Electrical Engineering,
University of Bath, Claverton Down,
Bath, BA2 7AY, United Kingdom.
{S.Rakshit, D.M.Monro}@bath.ac.uk

Abstract—We present a method for selecting good quality iris images from a sequence based on the position and quality of the specular reflection relative to the pupil. Using a simple low complexity yet robust technique, fast image selection is achieved along with immediate iris localization. Initial screening is achieved by accepting images with appropriate specular reflection intensity, width, height and area. Finer selection is then based on graylevel changes between light-pupil and pupil-iris regions. The method has been evaluated on numerous problem images and all were correctly rejected. Connected-component algorithms are used to find exact pupil boundaries and iris edges are modeled by ellipses based on left-right segmented boundaries. On a test set of 400 classes consisting of over 60000 images, no false acceptances are noted.

Keywords—Iris Quality, Localization, Connected Components.

Topic area—Biometrics.

I. INTRODUCTION

Image quality plays a crucial role in any pattern matching system. This is all the more evident in the case of biometric [1], and iris recognition in particular [2, 3], where verification performance is totally based upon matching fine texture information in the thin annular region between the pupil and the sclera. Yet, image acquisition and selection has oft been an area of limited activity with most research focusing on better localization and feature extraction techniques to improve recognition performance. Needless to say a transform is only as good as the data that is fed into it and with proper image screening all classifiers can achieve a dramatic improvement in accuracy.

Most previous work in this area has dealt with Quality as an independent topic separate from the localization process. In his pioneering work, Daugman used the high frequency energy of the Fourier transform to determine the sharpness of the iris image [4]. Zhu et. al. evaluated iris image quality by analyzing the coefficients of particular areas of iris texture by employing discrete wavelet decomposition [5]. Ma et al. analyzed the Fourier spectra of local iris regions to characterize defocus, motion and occlusion [6]. In all the above cases quality evaluation has been achieved using one or two factors without providing for an overall system. Recently significant advances in this area have been made by Kalka et. al. [7] and Chen et. al. [8]. Both groups have taken a more

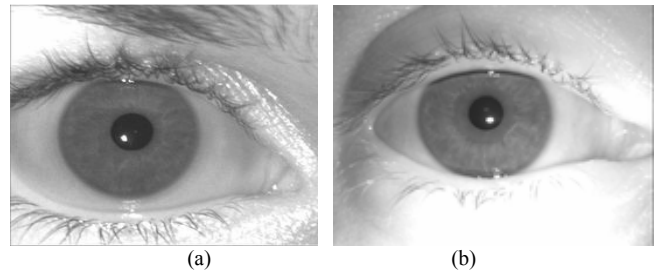


Fig. 1. Sample images from (a) LG and (b) Securimetrics Iris recognition systems.

global approach towards determining the overall quality of the iris image.

Here we propose a simple yet robust coarse-to-fine method of screening an image sequence rather than produce a complex figure of merit for each image. Despite the latter having its own applications, it is generally the former which is of primary concern during real-time operations. During image acquisition the subject moves back and forth, sideways, blinks or looks away. He may move his head, eyes or both. All these cases give rise to non-ideal images which may be difficult to normalize and match. At present many systems take the whole image sequence and compare them against the whole database looking for a match as the probability of a false acceptance is very low. This approach is not only time consuming but also prone to errors, especially as the database size grows to comprise national and international populations.

Screening during capture is the best solution to both these problems. Since image capture is generally carried out at the rate of 15 to 30 frames per second, individual frame analysis and localization can be done in real time thereby eliminating the need for whole video sequence storage and comparison. Depending upon system requirements, the best N images from the whole sequence can be stored and coded per eye. N would generally be an odd number of images, and is commonly taken as 3 whose average matching score is taken for comparisons.

Most present day systems including that by LG and Securimetrics restrict their light source to the pupil region while acquiring iris images for verification and identification as shown in Fig. 1. While providing a more uniform illumination this does not cause any loss in iris texture by obscuring it. Thus a gross-level screening can be achieved based simple on the position and size of the specular reflection

in the eye. If necessary, a finer evaluation can then be carried out using graylevel-change analysis before a decision is reached whether to proceed with localization or not. Upon successful localization, the matcher can be called with the N best images providing for a more accurate reduced-set identity verification setup.

The paper is subdivided into the following sections. Section 2 illustrates the various problem images encountered during image acquisition. The proposed selection technique along with localization details are elaborated on in Section 3. Results from over 60000 images are shown in Section 4 along with detailed graphs. Finally, Section 5 concludes the paper with conclusions and suggestions for future work.

II. PROBLEM IMAGES

The most common problems that arise in eye images during acquisition are occlusions, motion-blur, defocus and off-angle. Occlusions occur when the subject blinks during image capture. In that case the eye may be partially or fully covered by eyelids. This may also lead to motion blur which is generally a direct consequence of head tilt or eye movement. As the subjects move towards or away from the camera the image of the iris comes into focus and then gets blurred again. As the amount of defocus increases, the area of the light increases with it.

For small depth-of-field lenses, this situation arises often as a slight movement from the region around the focal plane causes serious blurring of the entire image. Additionally, partial out-of-focus problems may arise when the eye looks away from the direct line of sight of the camera-lens. In that case, one part of the iris may be in focus while the other is not. Looking away from the straight path also gives rise to off-angle images. In the event of lack of adequate number of good images from the entire video sequence, these off-angle images may be accepted and mapped back to rectangular coordinates if the overall focus and illumination is retained. A sample set of all these problem images is shown in Fig. 3.

III. PROPOSED SELECTION TECHNIQUE

The selection procedure is started by first subsampling the images to a resolution of 160×120 , one-quarter of the usual 640×480 sized images captured. This helps reduce

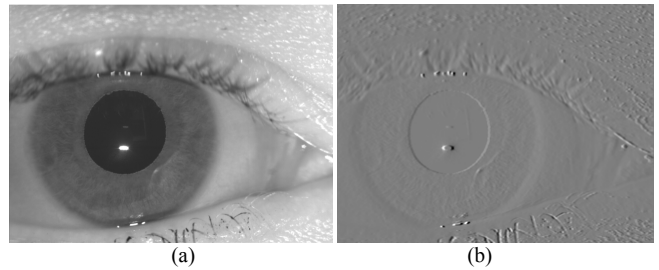


Fig. 2. a) Original Image, b) Graylevel difference image taken over 5 pixel wide regions.

computational complexity without loss of essential information relevant for specular reflection statistics measurements in either direction. Horizontal line graylevel difference analysis is then carried out, summed over 5-pixel-wide regions. This is done to better observe gradual changes between pupil-iris and iris-sclera boundaries which are often gradual changes rather than sharp jumps. The resultant image from the above graylevel difference analysis is shown in Fig. 2b.

The grouped changes are then globally sorted in descending order in an array, say P_kChng , and the top one taken. This is compared against the minimum allowed cutoff, set at 165, and if found to be lower than that, the image is rejected. This simple step helps screen out most images with specular reflections outside the pupil region along with blink-affected eyes as a low change in graylevel indicates it did not happen between two extremes, dark pupil to bright light.

Having passed the first stage, the pixel location is noted and assumed to be the starting point of the specular reflection in the pupil. The row, say P_kRow , is then scanned forwards and length of the first series of contiguous pixels with graylevel greater than 200 taken as the light width checked against permissible width boundaries. If found to be outside the allowed band, the ongoing analysis is aborted and a new one started with the next highest graylevel rise, $P_kChng(2)$. This helps screen out wrongly located light positions, generally caused in the dark eyelash regions. The width of the specular reflection in this case is not likely to be within the range as expected in the pupil zone. A *count* is kept and incremented every time the sequence is restarted and the

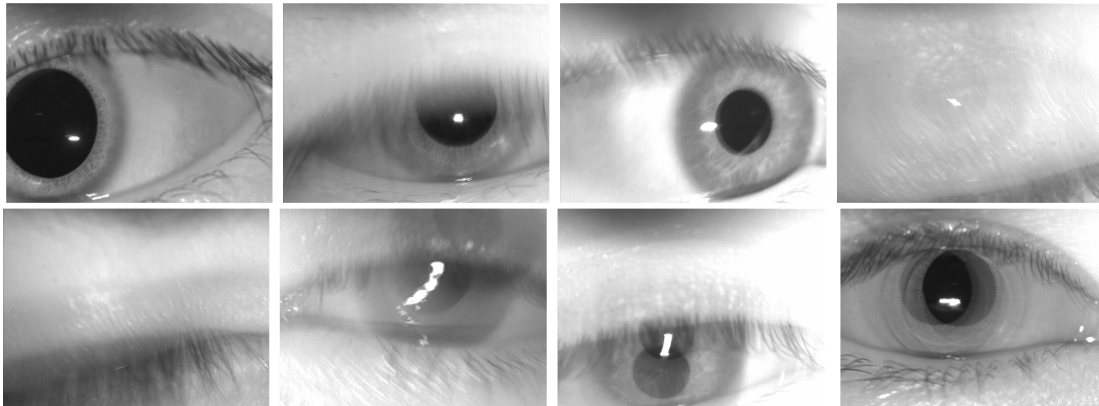


Fig. 3. Eye Images taken from video sequences depicting various issues faced during acquisition. This may be caused due to eye/head movement, blinking, etc.

image rejected if the *count* reaches 5 with no success.

The light-to-pupil change in graylevel, over a 5 pixel region, is evaluated and compared against a minimum cutoff to check if the light is at the edge of the iris. This situation generally arises when the eyeball moves out of the direct line-of-sight from the lens leading to partial or total blurring. It may also arise due to the presence of an artificial lens in the eye, which gives rise to multiple specular reflections in the pupil. Based on the latter assumption the image is not rejected at this stage and the procedure restarted to search for the next reflection position in the pupil. The *count* is incremented again.

With the specular reflection location within the pupil determined with considerable accuracy, a column of pixels centered at the middle of the light-width is taken and the light height measured as the length of the contiguous column with grayvalues greater than 200. This is then compared against the expected height range and similar action taken as in for light-width analysis done before. Following this, an adaptive approach is taken to set the light and pupil region cut-off thresholds. The median grayvalue of four pixels around the light-to-pupil transition region is used as a threshold to binarize the image and the area of the connected-components starting from the centre of the light is measured. This gives the area of the specular reflection as shown in Figs. 4a. and b, and if found to be greater than the maximum expected value, the image is rejected. At this stage, most defocused and motion-blurred images get rejected.

The pupil threshold is similarly found by taking the median value of four pupil points around the reflection but further than before. The original image is again binarized and

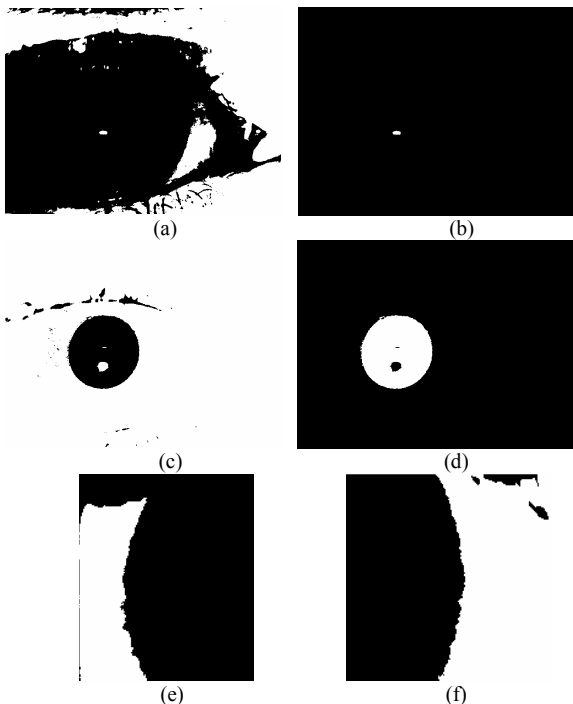


Fig. 4. (a) Binarized image for threshold based on bright light spot; (b) Bright Spot area; (c) Binarized image for threshold based on pupil grayvalues; (d) Pupil Area; Iris segment edges – (e) Left, and, (f) Right.

the pupil boundaries located using a connected components method starting from a point on the inside as illustrated in Figs. 4c. and d. In order to get a perfect pupil edge and eliminate all ‘holes’ within it a ‘noholes’ approach is taken during boundary detection. If the boundary is found to coincide with the image edges at any point, the image is rejected in order to eliminate out-of-line-of-sight cases. Modal curvature of the boundary is calculated by taking three points at a time spread over its circumference. Points deviating beyond $\pm 5\%$ from this value are removed and replaced by ones calculated using a straight line equation connecting its two nearest neighbors. The last stage of image rejection checks the pupil-to-iris transition and compares it against a minimum cutoff in order to eliminate images with a shadowy effect at this boundary which is a direct consequence of fast sideways eye movement during capture.

Starting with the pupil edges on the left and right, the iris boundary is searched for on either side. The top and bottom segments are mostly found to be occluded by eyelids and eyelashes thereby giving rise to spurious edges. Scanning outwards from the centre along the mid-row of this region, say R_m , the sclera is reached on either side after the first graylevel change greater than a preset cutoff. Median values of four points around these regions are obtained separately and used to binarize the image segments individually as shown in Figs. 4e. and f. Resultant edge points are further screened by eliminating points outside a band around the column centered around the intersection of the iris edge with the mid-row, R_m . An ellipse is then fitted to the remaining points to model the iris boundary. The entire procedure is illustrated in the flowchart in figure 6.

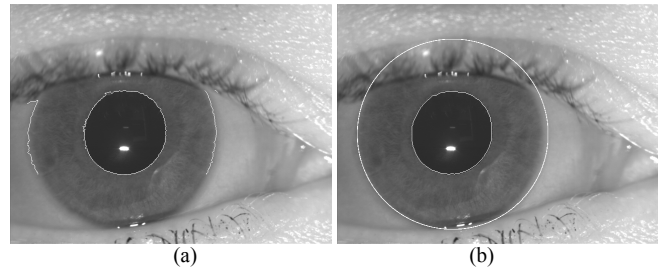


Fig. 5. a) Initial - Gross, and b) Final - Fine Localization

IV. RESULTS

As part of our ongoing research efforts into building the largest publicly available iris image database in the world, we have collected and stored video sequences from over 200 subjects from a variety of backgrounds [9]. 150 frames are captured from each eye producing a total of 60000 images taken under infrared lighting with a resolution of 1280x960. Longer video sequences are captured for subjects with handicaps or other difficulties.

The entire collection of images was passed through the preselection process and the various parameters, such as boundary change cut-offs and specular reflection width, height and area were set. The successful ones were checked manually for quality and the failed images studied to confirm that good images have not been rejected. No such instances were observed in either case.

V. CONCLUSIONS

In this paper, we have presented a simple, fast yet robust method of selecting good quality iris images from any given eye image video-sequence based on the position and quality of the specular reflection relative to the pupil. The low complexity of the illustrated procedure helps achieve real-time on-the-fly image screening without imposing additional overheads on the system.

The incorporation of accurate pupil and iris boundary localization makes the procedure more appealing. Better screening procedure helps cut down matching times dramatically as only a small fraction of images need to be coded. Storage requirements can also be brought significantly as the best N images from the sequence saved for later offline evaluation.

Many aspects of this method remain unexplored. Accurate iris focus evaluation, better pupil and iris boundary modeling and inclusion of light-outside-pupil images remain to be studied.

ACKNOWLEDGMENT

This work was sponsored by Smart Sensors Limited, Portishead, Bristol BS20 7BA, United Kingdom.

REFERENCES

- [1] M. Gamassi, M. Lazzaroni, M. Misino, V. Piuri, D. Sana, and F. Scotti, "Quality assessment of biometric systems: a comprehensive perspective based on accuracy and performance measurement," *Instrumentation and Measurement, IEEE Transactions on*, vol. 54, pp. 1489-1496, 2005.
- [2] J. Daugman, "The importance of being random: Statistical principles of iris recognition," *Pattern Recognition*, vol. 36, pp. 279-291, 2003.
- [3] R. P. Wildes, "Iris recognition: an emerging biometric technology," *Proc. of the IEEE*, vol. 85, pp. 1348 - 1363, 1997.
- [4] J. Daugman, "High confidence visual recognition of persons by a test of statistical independence," *IEEE Trans. on Pattern Analysis and Machine Intelligence*, vol. 15, pp. 1148 - 1161, 1993.
- [5] X.-D. Zhu, Y.-N. Liu, X. Ming, and Q.-I. Cui, "A Quality Evaluation Method of Iris Images Sequence Based on Wavelet Coefficients in "Region of Interest", presented at The Fourth International Conference on Computer and Information Technology (CIT'04), 2004.
- [6] L. Ma, T. Tan, Y. Wang, and D. Zhang, "Personal identification based on iris texture analysis," *IEEE Trans. on Pattern Analysis and Machine Intelligence*, vol. 25, pp. 1519 - 1533, 2003.
- [7] N. D. Kalka, V. Dorairaj, Y. N. Shah, N. A. Schmid, and B. Cukic, "Image Quality Assessment for Iris Biometric," presented at The Biometric Consortium Conference, Arlington, USA, 2005.
- [8] Y. Chen, S. C. Dass, and A. K. Jain, "Localized Iris Image Quality Using 2-D Wavelets," *Lecture Notes in Computer Science*, vol. 3832, pp. 373 - 381, 2005.
- [9] "University of Bath Iris Image Database, <http://www.bath.ac.uk/elec-eng/pages/sipg/irisweb/>."

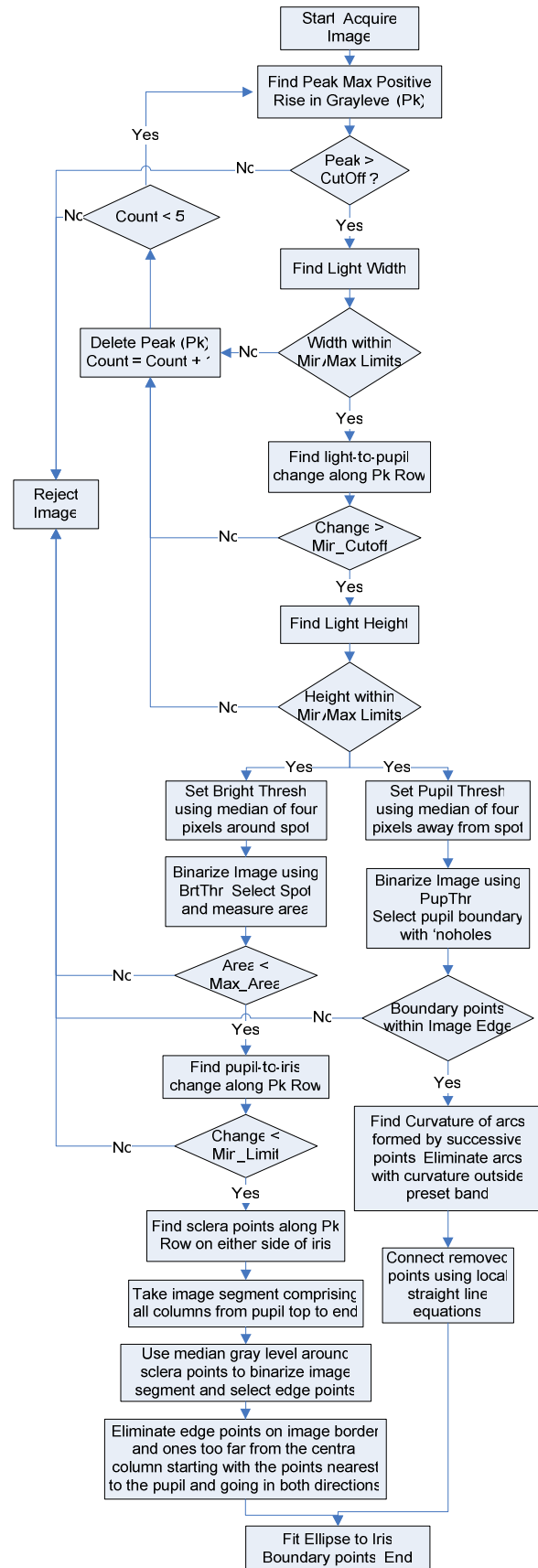


Fig. 6. Illustrating the various steps in iris image screening and localization